Measurements of Microwave Emission from a Foam-Covered, Wind-Driven Sea

W. NORDBERG, J. CONAWAY, DUNCAN B. ROSS[1] AND T. WILHEIT

Goddard Space Flight Center, Greenbelt, Md.

(Manuscript received 13 October 1970, in revised form 11 January 1971)

ABSTRACT

Measurements were made from aircraft of the 1.55-cm microwave emission from the North Sea and North Atlantic at surface wind speeds ranging from less than 5 to 25 m sec^{-1}. Brightness temperatures in the nadir direction increased almost linearly with wind speed from 7 to 25 m sec^{-1} at a rate of about 1.2C $(m\ sec^{-1})^{-1}$. At 70° from nadir the rate was 1.8C $(m\ sec^{-1})^{-1}$. This increase was directly proportional to the occurrence of white water on the sea surface. At wind speeds <7 m sec^{-1}, essentially no white water was observed and brightness temperatures in the nadir direction were ~120K; at wind speeds of 25 m sec^{-1} white water cover was on the order of 30% and average brightness temperatures at nadir were ~142K. Maximum brightness temperatures for foam patches large enough to fill the entire radiometer beam were 220K.

1. Introduction

Considerable interest has been devoted to the quantitative measurement of sea surface roughness, on a global scale, from spacecraft and to the possible derivation of surface winds from these measurements (NAS Summer Study, 1969). For this reason, we measured the microwave emission at 1.55 cm over the North Atlantic and the North Sea in March 1969 over a wide range of sea surface, wind and cloud conditions in order to establish a quantitative relationship between the emission and the sea state and to delineate parameters such as surface winds, foam cover, wave height and cloud cover that would affect this relationship.

Earlier measurements (Nordberg *et al.*, 1969) over the Salton Sea have shown that the microwave emission, observed at all nadir angles from 0° to 50° and at a wavelength of 1.55 cm, is considerably greater from a rough water surface than from a smooth one. Stogryn (1967) had predicted that increases in microwave emission from rough water could be observed only at nadir angles $>30°$. However, Stogryn's calculations were addressed primarily to the effect of the large-scale wave geometry on the emission and did not, for example, account for foam and spray. We have therefore conducted these observations at high wind speeds and extensive foam cover to investigate further this discrepancy between theory and earlier observations.

2. Description of experiment

Measurements were made from the NASA Convair 990 airborne observatory. Primary instruments carried by the aircraft were as follows:

1) A radiometer measuring horizontally polarized radiation at 1.55 cm wavelength within a 2.8° diameter field of view which was scanned perpendicularly to the aircraft's flight path over a nadir angle range of ±50°. The same instrument was used in the Salton Sea observations; it was built by the Space Division of Aerojet General Corporation (Oister and Falco, 1967).

2) A laser geodolite of the Spectra-Physics Corporation to measure the ocean wave height spectrum.

3) An infrared radiometer, similar to the Medium Resolution Infrared Radiometer (MRIR) flown on Nimbus satellites (*Nimbus III User's Guide*, 1969), to determine the sea surface temperature from emission measurements at wavelengths between 10.6 and 11.6 μm.

4) Standard airborne navigation systems, both Doppler and inertial, with which wind speed and direction at the aircraft altitude were measured.

5) A Vinton 70-mm camera, pointing at nadir with a square field of view of about 68°, to photograph sea surface and cloud conditions.

In addition, the aircraft carried standard instrumentation for altitude, attitude, speed, and ambient temperature measurements and auxiliary cameras. A nonscanning, nadir viewing, 3-cm microwave radiometer with a field of view of about 13°×13° was provided by the Jet Propulsion Laboratory for comparison with the 1.55-cm measurements.

The aircraft was based at Shannon, Ireland. Two flights, averaging 5 hr each, were made over the North Sea, and four flights, equally long, covered a region of the North Atlantic between Iceland and Ireland. In general, passes were made over each area of interest at several altitudes between 120 and 12,000 m to differentiate the effects of atmospheric and surface emission.

[1] Present affiliation: NOAA Air-Sea Interaction Laboratory, Miami, Fla.

TABLE 1. Summary of meteorological conditions and microwave emission temperatures for six overwater flights.

	Case					
	A	B	C	D	E	F
Date (March 69)	10	13	13	10	19	14
Time (GMT)	1321	1247	1117	1430	1023	1453
Location	Atlantic Off Shannon	Atlantic Ship J	Atlantic Ship I	Atlantic Ship I	North Sea 57°N 3°E	North Sea 59°N 1°30′E
Wind speed (m sec^{-1})	<5	6	13	16	17	25
Significant wave height (m)	<1	6.0†	3.9	5.0	4.0	7.8
Foam cover (%)						
Whitecaps	—	—	4.2	5.6	6.0	5.0
Streaks	—	—	3.5	6.9	17.4	27.0
Total	—	—	7.7	12.5	23.4	32.0
Temperature (°C)						
Sea surface	9	10	9	9	2	4
Air surface	10 (est.)	11	7	5	2	2
Cloud altitude (m)						
Base	2000	clear	300	800	600	150
Top	2300	clear	2100	2000	2000	5000
Brightness temperature (°K)						
High altitude*	128**	—	—	138	138	148
Low altitude	120	118	127	132	132	142

* Measured within 30 min of time shown.
** Over Irish Sea at 1212 GMT.
† All swell, no wind waves.

Surface wind speeds ranged from calm to 25 m sec^{-1}. They were obtained from surface anemometer observations and/or by extrapolation of the aircraft measured ambient wind speeds at the lowest flight altitudes under the assumption that wind speed decreased exponentially toward the surface (Ross *et al.*, 1970). Where both were available no significant discrepancy was noted. This assumption was applied to all cases shown in Table 1, except case E. In that case, examination of reduced geostrophic winds and ship reports led us to assume that the wind speed *increased* from the height of the aircraft to the surface. We are very much indebted to Prof. Vincent Cardone of New York University for pointing this out to us. A similar increase in wind speed with decreasing altitude was observed during the Salton Sea flight. However, in the absence of surface observations, it was not deemed appropriate to depart from the winds observed at 200 m, the minimum aircraft altitude, for our approximation of the surface winds. In this case, it is recognized that the true surface wind speed could be considerably higher. For the Atlantic Ocean and North Sea observations, the accuracy of the surface wind speed determinations is judged to be within 3 m sec^{-1}.

Cloud conditions, observed visually and photographically from the aircraft, ranged from clear to stratocumulus overcasts with moderate rain, over the numerous sea surface targets selected for the flights.

The 10–11 μm equivalent blackbody temperatures were taken to be equal to the sea surface temperature when measured with the infrared radiometer at the lowest altitudes. Temperatures ranged from 10C at 50N over the Atlantic to 2C over the coldest part of the North Sea.

Sea state varied from calm, with no whitecaps, to significant wave heights of ~8 m with over 30% coverage by foam with extensive streaking. Significant wave heights were determined by analysis of the wave spectra observed with the laser geodolite. The foam coverage was determined from photographs of the sea surface with a digital densitometer. The method consists of numerically computing the areas on the photographs above and below a chosen brightness threshold such that whitecaps, foam streaks and undisturbed sea can be differentiated quantitatively. These parameters are listed in Table 1. Due largely to the subjective nature of the choice of the thresholds, the accuracy of this method is limited to about 15% of the value obtained. Percentages for each case are averages resulting from several consecutive photographs due to the variation in the foam cover between individual frames.

Whenever possible, sea state, temperatures and winds measured with the aircraft were compared with the observations obtained from ocean vessels I and J (59N, 19W and 53N, 20°30′W, respectively) and with analyses made by the Irish Meteorological Service at Shannon Airport. There was never any significant discrepancy among these data. A complete log of all flights, including environmental and meteorological observations was compiled by Griffie *et al.* (1969). The specific conditions for which microwave measurements are reported here are summarized in Table 1.

3. Results

Brightness temperatures measured at 1.55 cm during six low-altitude passes over the Atlantic and North Sea at wind speeds ranging from less than 5 to about 25 m sec^{-1} were selected to illustrate their dependence on

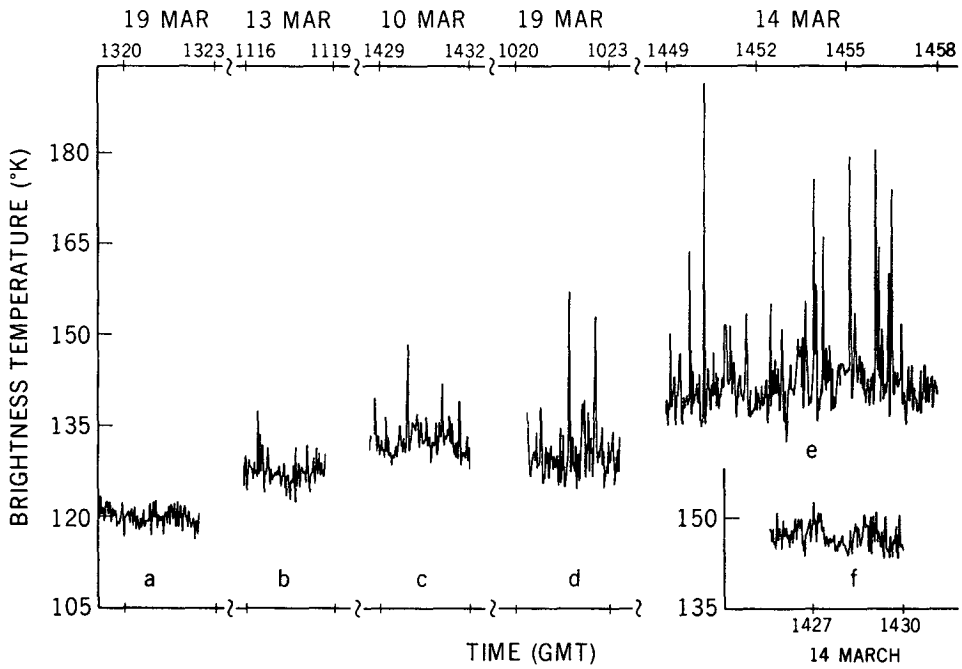

FIG. 1. Instantaneous brightness temperatures measured in the nadir direction vs time. Plot (a) corresponds to case A in Table 1, plots (b)–(e) to cases C–F. All brightness temperatures in (a)–(e) were observed from heights of ~150 m. Brightness temperatures in (f) were observed from a height ~5500 m over approximately the same location as (e).

wind speed and foam cover (Fig. 1). The recorded radiometer output was converted to radiances taking into account the calibrations performed on board the aircraft during each scan with two reference loads, one stabilized at 330K and another terminated in a liquid nitrogen dewar. Antenna and radiometer characteristics, including effects of radiation received by the antenna through side lobes outside the 2.8° diameter instantaneous field of view which were measured in the laboratory and against a known sky background prior to and after the expedition, were also taken into account in this conversion. The resulting radiances are expressed as brightness temperatures (°K) and are plotted in Fig. 1 for the nadir viewing positions only. The radiometer field of view scanned from 50° left of nadir to 50° right of nadir, once every 2 sec. Thus, the traces shown in Fig. 1 consist of one data point per 2 sec. They cover time segments corresponding to the sea, cloud and wind conditions listed in Table 1.

The plotted brightness temperatures (T_B) result from three radiation components received by the radiometer—radiation emitted to the aircraft by the sea surface, radiation emitted to the aircraft by clouds and atmospheric water vapor, and atmospheric radiation reflected toward the aircraft by the sea surface:

$$T_B = \epsilon T_W \tau_H + (1-\epsilon) T_S \tau_H + \int_0^H T_A(h)(\partial\tau/\partial h)dh, \quad (1)$$

where T_W is the water surface temperature, T_S the sky brightness temperature, T_A the atmosphere temperature, τ the atmosphere transmissivity, ϵ the surface emissivity, h height above surface, and H aircraft altitude. The first, second and third terms of (1) correspond to surface emission, reflected atmospheric radiation, and atmospheric emission, respectively.

The cases listed in Table 1 were chosen such that atmospheric conditions, including cloud cover, were generally similar. In each of these cases, there was no measurable precipitation from the prevailing broken stratocumulus clouds. Somewhat denser cloud cover encountered during higher wind speeds was almost compenstated for by the lower atmospheric temperatures prevailing in these cases. For example, we have computed that the reflected radiation component for cases A and B of Table 1 (thin clouds but warm atmosphere) contributed ~9.5C to the measured brightness temperature, while for cases E and F (thicker clouds, but cold atmosphere) this contribution was ~11C. Thus, for the conditions listed in Table 1, the reflected component due to T_S can be assumed to be nearly constant, with variations certainly remaining smaller than 3C. Also, the directly received emitted atmospheric radiation was negligible when the aircraft was at low altitudes (150–200 m), since there were no clouds below the aircraft, and the transmissivity was very near unity between the aircraft and the surface. In those cases, the integral term in Eq. (1) approaches zero.

Measurements of T_B were also made from high altitudes (>5000 m) for the same conditions and gener-

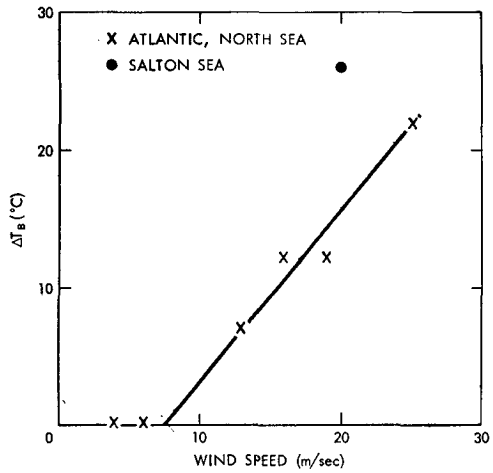

FIG. 2. Brightness temperature differences between observations made at wind speeds <5 m sec^{-1} and higher wind speeds as a function of wind speed.

ally within less than 30 min of the times listed in Table 1. Brightness temperatures were 6–8C higher (depending on sea surface roughness) than corresponding brightness temperatures observed at the low altitudes. In each case, these increases relative to the low-altitude passes account quite precisely for the emitted atmospheric radiation term and for the decrease of τ_H from unity to about 0.95. The comparison between low- and high-altitude observations confirms our assertion that the measurements shown in Fig. 1 were obtained under comparable atmospheric and cloud conditions.

At this wavelength, the measured brightness temperatures are essentially independent of the sea surface temperatures within the observed range, because ϵ varies inversely with the surface temperature such that ϵT_W in Eq. (1) is nearly constant. Differences between the measured brightness temperatures for the various cases of Table 1 are then almost entirely due to differences in sea surface roughness. Brightness temperature differences between the lowest wind condition (case A) and each of the other cases were computed and plotted vs surface wind speeds in Fig. 2. A systematic increase in emission with increasing wind speed is clearly evident. The rate of increase is ~1.2C (m sec^{-1})$^{-1}$. A qualitatively similar result was obtained from the data taken over the Salton Sea in 1968. This previously unpublished datum is from the same series of measurements discussed by Nordberg *et al.* (1969). The apparent quantitative disagreement with the 1.2C rate of increase for the North Atlantic and North Sea measurements is not deemed significant because of the large wind speed uncertainty in the Salton Sea case.

Measurements for the nadir direction only were plotted in Figs. 1 and 2. At larger nadir angles, up to 70°, we have observed proportionally larger rates of increase. Fig. 3 shows brightness temperatures as a function of nadir angle for a low and for the highest wind speeds listed in Table 1. Although the radiometer antenna scanned only to nadir angles up to 50°, we were able to observe radiation from nadir angles up to 80° during banking of the aircraft. The two solid curves in Fig. 3 were obtained by smoothing brightness temperature averages at each nadir angle for periods of 10–20 sec during which the aircraft bank angle was held constant at 30°. The brightness temperature rate of change with wind speed increased from 1.2C (m sec^{-1})$^{-1}$ at nadir to ~1.8C (m sec^{-1})$^{-1}$ at 70° from nadir. This is qualitatively in accord with observations by Hollinger (1970), who reported an increase from 0.8C (m sec^{-1})$^{-1}$ at 30° from nadir to 1.4C (m sec^{-1})$^{-1}$ at 70° from nadir, for a much lower wind speed range.

The dashed curve in Fig. 3 was computed for the atmospheric and sea surface temperature conditions observed for case B, but for a specular sea surface. The absolute brightness temperatures measured at nadir for case B were ~15C lower than the computed temperatures (dashed curve). We believe that this discrepancy is largely due to errors in the *absolute* calibration of the radiometer and indicates that all brightness

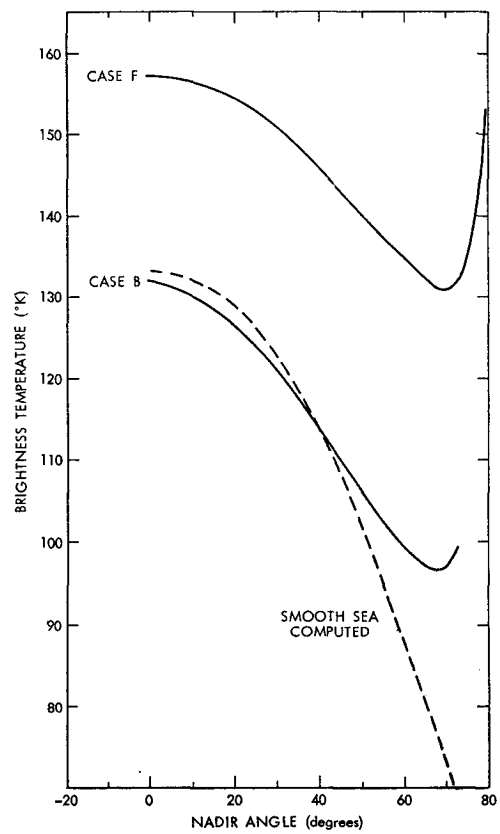

FIG. 3. Brightness temperatures averaged for 10–29 sec time periods, for each antenna scan angle during 30° aircraft banks, vs nadir angle for case B of Table 1 (lower curve) and case F of Table 1 (upper curve). Absolute brightness temperatures were normalized to computations for smooth sea (dashed curve) at nadir. The dashed curve shows computed brightness temperatures for atmospheric and sea surface temperatures encountered in case B but for a smooth, specular sea surface.

temperatures measured with this instrument should be corrected by about +15C. This correction was made for the brightness temperatures plotted for cases B and F in Fig. 3. The relative calibration of the instrument was maintained at about ±1.5C throughout all flights.

Comparison of the slope of the dashed curve with the slope of curve B shows that the decrease of brightness temperatures with nadir angle is much steeper for a theoretical, specular and smooth water surface than for real water surfaces, even at low wind speeds. This suggests that the small-scale roughness introduced even by very low winds causes a considerable brightness temperature increase at large nadir angles. The slopes of curves B and F differ much less than those of curve B and the smooth water curve. This suggests that the rate of brightness temperature increase with nadir angle diminishes at the higher wind speeds. However, there remains a brightness temperature increase of at least 22C with wind speed at all nadir angles, as shown by the offset of curve F compared to curve B. This offset could be caused by the greater emission from white water such as foam and spray which would produce nearly the same brightness temperature increase at all nadir angles, depending only on the amount of foam cover.

Fig. 2 shows that a nearly linear brightness temperature increase with wind speed occurs above a threshold of ~7 m sec^{-1}. The measurements at 6 m sec^{-1} (case B) show no increase of T_B over the measurements at less than 5 m sec^{-1} (case A). There is no evidence of any brightness temperature difference between cases A and B despite the fact that the sea surface was very smooth for case A while extremely large swells (6 m) but no whitecaps were observed for case B. Monahan (1969a) has reported an abrupt increase in whitecap coverage and spray density at 7 m sec^{-1} and Cardone (1969) has computed that the energy available for whitecap production at wind speeds <7 m sec^{-1} is practically negligible. This suggests that the increase of microwave emission with wind speed, shown in Fig. 2, is related mainly to the occurrence of white water (foam and spray). At lower wind speeds, where foam does not occur, the brightness temperature measured at all nadir directions is independent of wind speed. Foam has been suspected previously as a cause for increased microwave emission (Williams, 1969; Droppleman, 1970).

Further evidence of the dependence of the microwave emission on foam cover can be found in the rapid brightness temperature fluctuations with time, shown in Figs. 1c–1e. In Fig. 1d, for example, the average brightness temperature is ~132K, but, instantaneous spikes frequently reach 140K and two spikes exceed 155K. Fig. 1e, which corresponds to winds of 25 m sec^{-1}, shows many more of these spikes. In this case, the average brightness temperature is ~142K, but instantaneous spikes exceeding 150K occur about every 30 sec. Several of these spikes range between 175 and 190K. From the photographs there is a strong implication that these spikes are caused by foam patches on the sea surface.

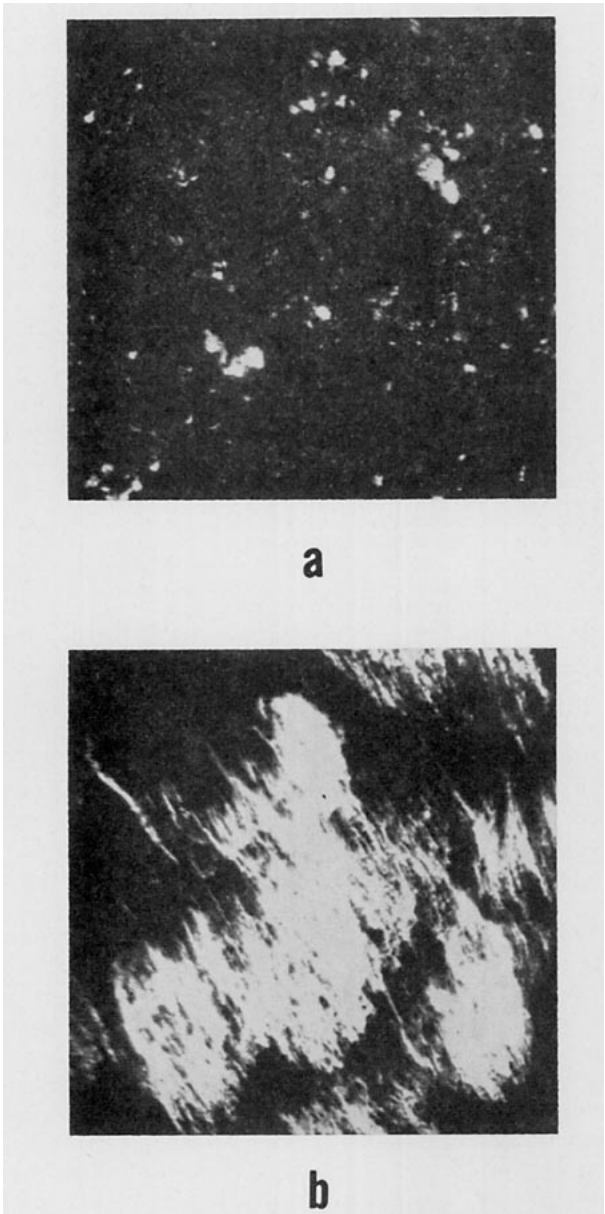

FIG. 4. Photographs with a 70-mm camera taken in the nadir direction at surface wind speeds of 16 m sec^{-1} (a) and 25 m sec^{-1} (b), corresponding to cases D and F, respectively, in Table 1.

We have analyzed the instantaneous brightness temperatures measured at all scan angles over a period of 20 min, approximately centered on the time corresponding to Fig. 1e. to determine the amplitude and frequency of brightness temperature spikes. We found that the maximum amplitude was ~220K for seven spikes which occurred during that period. One such spike was clearly coincident with the immense foam patch photographed in Fig. 4b. The radiometer scanned the scenes shown in Fig. 4 from left to right, with the

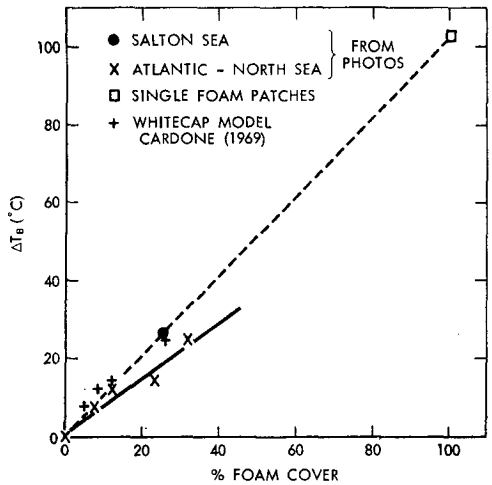

FIG. 5. Brightness temperature differences between observations made at wind speeds less than 5 m sec^{-1} and at higher wind speeds as a function of foam cover as estimated from photographs, from the analytical model of Cardone, and from single foam patches covering the entire microwave radiometer beam.

aircraft having flown from bottom to top. Since the position of the scans on the photographs are not known exactly, and since at low altitudes scans were not contiguous, the foam patches may not always have filled the antenna field of view entirely. We assume that this occurred only when the maximum brightness temperatures of 220K were measured.

The photographs of Fig. 4 were taken over sea states corresponding to the brightness temperature measurements in Figs. 1c and 1e, respectively. Aircraft altitudes ranged from 120 to 450 m. Fig. 4b was observed from 120 m and extends over about 200 m from top to bottom. The foam estimates (Table 1) were made from time series of photographs similar to those shown in Fig. 4. The increasing amounts of both foam patches and streaking with wind speed are quite apparent from Table 1. We assume that such streaking and foam patches, which were small relative to the radiometer field of view, raised the measured brightness temperatures uniformly throughout each scan, but that the largest patches of foam produced the temperature spikes which were more than 70C above the average. It is, therefore, very important that estimates of foam coverage, as they relate to the microwave emission, include the effect of both foam patches and streaking. This has been attempted with the estimates of total foam cover listed in Table 1.

The brightness temperature spikes seen in Figs. 1d and 1e were not observed when the aircraft was at higher altitudes, where each foam patch covered an area much smaller than that resolved by the instantaneous field of view of the radiometer. Fig. 1f shows brightness temperatures measured from 5500 m in the vicinity where the photograph of Fig. 4b and the measurements shown in Fig. 1e were made. No large spikes are evident in this case. At the aircraft height of 120 m (Fig. 1e) each scan spot covered an area with a diameter of ~7 m, while at the aircraft height of 5500 m (Fig. 1f) the diameter of the area covered was ~275 m. In the latter case, brightness temperatures show a much smoother pattern with no significant spikes because the characteristic diameter and spacing of the largest foam patches were less than ~100 m (Fig. 4b) and individual patches were not resolved by the radiometer.

Brightness temperature differences were plotted vs foam coverage in Fig. 5, as determined from the photographs (solid line). There is a similar increase of brightness temperature with foam cover, as there is with wind speed. However, the rate of increase obtained from the small-scale, single foam patch measurements, each representing 100% foam cover (dashed line), is considerably greater than the rate determined from the large-scale observations derived from the photographs for less than 40% foam cover (solid line). There are two possible explanations for this discrepancy:

1) The estimates of streaking which account for a large portion of the white water coverage as determined from the photographs (Table 1) are subjective, though internally consistent. Thus, foam cover as determined from the photographs may have been overestimated. This is also suggested by the fact that if foam cover is taken from Cardone's (1969) model, corrected for salt water after Monahan (1969b), brightness temperature increases are consistent with the rate obtained for 100% foam cover (dashed line) which is independent of the estimates made from the photographs. The uncertainty of estimating whitewater coverage from photographs and the possibility of overestimating foam cover has been pointed out recently by Blanchard (1971).

2) Another possibility is that the total white water estimates made from the photographs are correct but that the effect of the streaks on the microwave emission is smaller than the effect of the whitecaps which produce the 100% foam cover spikes. In this case, the agreement with Cardone's model would be purely coincidental. Further microwave measurements under controlled conditions of foam and streaking should resolve this point.

It is noteworthy that the Salton Sea measurements made on 5 June 1968 are generally consistent with the North Sea and Atlantic measurements with regard to brightness temperature dependence on both wind speed and on foam cover.

Preliminary results from the 3-cm radiometer, flown simultaneously with the other instruments, indicate that the brightness temperature increase at this wavelength is about 8C for a wind speed increase from calm to 13 m sec^{-1}. Beyond 13 m sec^{-1} there is only a negligible increase in brightness temperature. However, because of calibration uncertainties, the 3-cm measurements cannot be considered as firm as those at 1.55

cm. We are indebted to Messrs. F. Barath and J. Blinn of the Jet Propulsion Laboratory and A. Edgerton of Aerojet General Corporation for making this, as yet unpublished, information available to us.

4. Conclusions

There is a definite increase in the thermal emission at 1.55 cm from the sea surface with increasing wind speed. On the average, this increase amounts to about 22C in the nadir direction and 32C at 70° from nadir for a wind speed increase from 7 to 25 m sec^{-1}. For very low wind speeds, up to about 7 m sec^{-1} when foam cover is negligible, there is no increase in brightness temperatures. Compared to calm sea states, brightness temperatures are ~100C higher when foam patches covering the radiometer field of view are observed. We conclude that the increased emission at 1.55 cm from a wind-driven sea surface is primarily due to white water cover, while the effect of the wave slope geometry is negligible. The microwave emission at 1.55 cm from the sea surface is therefore a sensitive indicator of white water coverage and of wind speed at all nadir angles, at least to 50°.

We believe that an important parameter involved in the interaction between air and the sea surface, namely, the energy expended in the production of white water, can be inferred from microwave brightness temperature measurements provided that: 1) the consistent relationship between white water occurrence and wind speed reported here is confirmed; and 2) microwave measurements are made at various wavelengths, both polarizations, and over a large range of nadir angles to separate the various effects of foam cover, cloud cover, and atmosphere and sea surface temperatures on the microwave emission.

Results from the observations reported here might provide a basis to test further developments or revisions of analytical models relating microwave emission to sea surface roughness.

Acknowledgments. There were several dozen individuals without whom these observations would not have been possible. We are unable to name all of them, but we acknowledge their dedicated contributions gratefully. We are especially indebted to the NASA pilots and flight crew of the CV 990 observatory for carrying out the demanding flight operations that were required for these observations, to Mr. Earl Peterson of the NASA Ames Research Center for organizing the expedition, and the Irish Meteorological Service for providing excellent weather forecasts and analyses to support our flight operations.

REFERENCES

Blanchard, D. C., 1971: Whitecaps at sea. *J. Atmos. Sci.*, **27** (in press).

Cardone, V. J., 1969: Specification of the wind field distribution in the marine boundary layer for wave forecasting. Geophysical Science Lab., New York University, Rept. TR69–1.

Droppleman, J. D., 1970: Apparent microwave emissivity of sea foam. *J. Geophys. Res.*, **75**, 696–698.

Griffee, L., J. Ledgerwood, D. Hill and W. E. Marlatt, 1969: Support data for NASA Convair 990 meteorological flight IV. Dept. Atmos. Sci., Colorado State University, Ft. Collins, 83, pp.

Hollinger, J. P., 1970: Passive microwave measurements of the sea surface. *J. Geophys. Res.*, **75**, 5209–5213.

Monahan, E. C., 1969a: Freshwater whitecaps. *J. Atmos. Sci.*, **26**, 1026–1029.

——, 1969b: Laboratory comparisons of freshwater and salt water whitecaps. *J. Geophys. Res.*, **74**, 6961–6966.

NAS Summer Study, 1966. Useful applications of earth-oriented satellites. Summer study on space applications, National Academy of Sciences, Washington, D. C.

Nimbus III User's Guide, 1969: Staff Members, Nimbus Project, NASA, Goddard Space Flight Center, Greenbelt, Md.

Nordberg, W., J. Conaway and P. Thaddeus, 1969: Microwave observations of sea state from aircraft. *Quart. J. Roy. Meteor. Soc.*, **95**, 408.

Oister, G., and C. V. Falco, 1967: Microwave radiometer design and development. Final Rept., Contract NAS5-9680, Aerojet-General Corp., Space Division, El Monte, Calif.

Ross, D. R. V. Cardone and J. Conaway, 1970: Laser and microwave observations of sea surface conditions for fetch limited 35 to 50 knot winds. *IEEE Trans. Geoscience Electronics*, **GE-8** (in press).

Stogryn, A., 1967: The apparent temperature of the sea at microwave frequencies. *IEEE Trans. Antennas Propagation*, **AP-15**, 278.

Williams, G. F., Jr., 1969: Microwave radiometry of the ocean and the possibility of marine wind velocity determination from satellite observations. *J. Geophys. Res.*, **74**, 4591–4594.